

# Extremal statistics of curved growing interfaces in 1+1 dimensions

JOACHIM RAMBEAU<sup>1</sup> and GRÉGORIE SCHEHR<sup>1</sup>

<sup>1</sup> *Laboratoire de Physique Théorique (UMR du CNRS 8627), Université de Paris-Sud 11, 91405 Orsay Cedex, France*

PACS 05.40.-a – Fluctuation phenomena, random processes, noise, and Brownian motion

PACS 02.50.-r – Probability theory, stochastic processes, and statistics

PACS 75.10.Nr – Spin-glass and other random models

**Abstract.** - We study the joint probability distribution function (pdf)  $P_t(M, X_M)$  of the maximum  $M$  of the height and its position  $X_M$  of a curved growing interface belonging to the universality class described by the Kardar-Parisi-Zhang equation in 1 + 1 dimensions, in the long time  $t$  limit. We obtain exact results for the related problem of  $p$  non-intersecting Brownian bridges where we compute the joint pdf  $P_p(M, \tau_M)$ , for any finite  $p$ , where  $\tau_M$  is the time at which the maximal height  $M$  is reached. This yields an approximation of  $P_t(M, X_M)$  for the interface problem, whose accuracy is systematically improved as  $p$  is increased, becoming exact for  $p \rightarrow \infty$ . We show that our results, for moderate values of  $p \sim 10$ , describe accurately our numerical data of a prototype of these systems, the polynuclear growth model in droplet geometry. We also discuss applications of our results to the ground state configuration of the directed polymer in a random medium with one fixed endpoint.

**Introduction.** – The study of fluctuations in stochastic growth processes has attracted much attention during the last two decades [1, 2]. Such processes are ubiquitous in nature as they appear in various physical situations ranging from paper wetting to burning fronts or growing bacterial colonies. In many experimental settings the growth starts from a point like region (a seed) with a strong tendency to evolve towards the approximate spherical symmetry. Such examples include fluid flow in porous media, adatoms and vacancy islands on surfaces [3] but also biological systems such as tumors [4].

To describe such phenomena driven by a growing interface, several models have been studied, like the Eden model, polynuclear growth models (PNG) or ballistic deposition models, among others [2]. In 1 + 1 dimensions, it is widely believed that all these models belong to the same universality class as that of the Kardar-Parisi-Zhang (KPZ) equation [5, 6]. At time  $t$ , the width of the interface  $W_L(t)$ , for such a system of size  $L$ , behaves like  $W_L(t) \sim L^\zeta \mathcal{W}(t/L^z)$  with universal exponents  $\zeta = \frac{1}{2}$  and  $z = \frac{3}{2}$  [7]. In the growth regime  $t_0 \ll t \ll L^z$  (where  $t_0$  is a microscopic time scale) exact results for different lattice models have shown that the notion of universality extends far beyond the exponents and also applies to full distribution functions of physical observables [8–10]. In particular, the scaled cumulative distribution of the height field coincides with the Tracy-Widom (TW) distribution  $\mathcal{F}_\beta(\xi)$

with  $\beta = 2$  (respectively  $\beta = 1$ ) for the curved geometry (respectively for the flat one), which describes the edge of the spectrum of random matrices in the Gaussian Unitary Ensemble (respectively of the Gaussian Orthogonal Ensemble) [11]. Height fluctuations were measured in experiments, both in planar [12] and more recently in curved geometry in the electroconvection of nematic liquid crystals [13] and a very good agreement with TW distributions was found.

Here we focus on a prototype of these models, the PNG model [14], but our results hold more generally for curved growing interfaces in the KPZ universality class (see below). It is defined as follows. At time  $t = 0$  a single island starts spreading on a flat substrate at the origin  $x = 0$  with unit velocity. Seeds of negligible size then nucleate randomly at a constant rate  $\rho = 2$  per unit length and unit time and then grow laterally also at unit velocity. When two islands on the same layer meet they coalesce. Meanwhile, nucleation continuously generates additional layers and in the droplet geometry, nucleations only occur above previously formed layers. Denoting by  $h(x, t)$  the height of the interface at point  $x$  and time  $t$ , one thus has  $h(x, t) = 0$  for  $|x| > t$ . On the other hand, in the long time limit, the profile for  $|x| \leq t$  becomes circular  $h(x, t) \sim 2t\sqrt{1 - (x/t)^2}$  [15], but there remain height fluctuations around this semi-circle. A natural way to characterize these fluctuations is to consider the maximal height

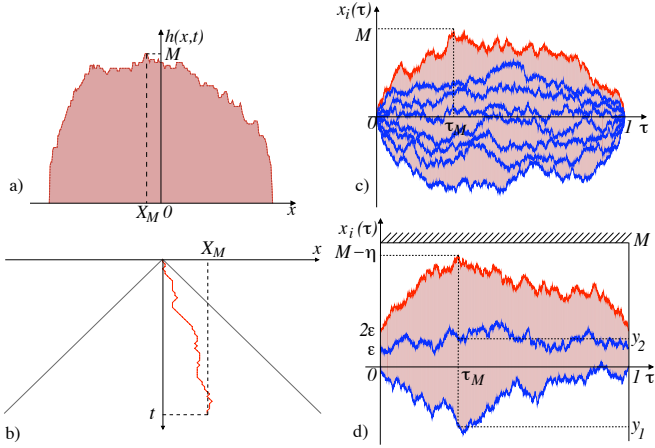


Fig. 1: **a)**: Height profile  $h(x,t)$  for fixed time  $t$  for the PNG model. **b)**: An optimal path of the DPRM of length  $t$ . **c)**: A  $p$ -watermelon configuration ( $p = 8$ ). **d)**: Sketch of the method to compute the joint pdf  $P_p(M, \tau_M)$ .

$M$  and its position  $X_M$  (see Fig. 1 a)). According to KPZ scaling, one expects  $M - 2t \sim t^{\frac{2}{3}}$ , while  $X_M \sim t^{\frac{2}{3}}$  [16]. The purpose of this Letter is to provide an analytic approach to the joint pdf  $P_t(M, X_M)$  for large  $t$ .

The PNG model can be mapped onto the directed polymer in a random medium (DPRM) on the square lattice with one fixed end [2,10]. In this language  $M$  is the ground state energy while  $X_M$  is the transverse coordinate of the free end of the optimal polymer of length  $t$  (see Fig. 1 b)). Related questions for the continuum DPRM are currently under active investigations [17]. The marginal distributions of  $M$  and  $X_M$  are already interesting and related extreme value quantities, like the maximal relative height, have been extensively studied in the stationary regime  $t \gg L^z$  [18–20]. Much less is known in the growth regime which we focus on. From the mapping onto the DPRM, one identifies the pdf of the maximal height  $M$  in the droplet geometry with the pdf of the height  $h_{\text{flat}}(x,t)$  at a given point  $x$  and time  $t$  in the planar geometry [21]. Therefore we conclude that the pdf of  $M$ , suitably rescaled and shifted, is given by  $\mathcal{F}'_1(\xi)$  [16, 22], the TW distribution for  $\beta = 1$ . On the other hand, the computation of the (marginal) distribution of  $X_M$  is a challenging open problem [16].

To compute  $P_t(M, X_M)$ , we exploit the exact mapping between the height field in the PNG model and the top path of  $p$  non-intersecting random walkers, so called vicious walkers [23], in the limit  $p \rightarrow \infty$  [8, 24]. Here we consider “watermelons” (Fig. 1 c)) where  $p$  non-colliding Brownian motions  $x_1(\tau) < \dots < x_p(\tau)$  on the unit time interval are constrained to start and end at 0 (*i.e.* Brownian bridges). In the large  $p$  limit, one can show, using the connection between this vicious walkers problem and random matrix theory, that  $x_p(\tau)$  also reaches a circular shape of amplitude  $\sqrt{p}$ ,  $x_p(\tau) \sim 2\sqrt{p}\sqrt{\tau(1-\tau)}$  while the

fluctuations are in that case of order  $p^{-\frac{1}{6}}$  [25]. Hence  $x_p$  and  $\tau$  map onto  $h$  and  $x$  in the growth model while  $p$  plays the role of  $t$ . This mapping, for  $p, t \gg 1$  reads [8, 24]

$$\frac{h(ut^{\frac{2}{3}}, t) - 2t}{t^{\frac{1}{3}}} \equiv \frac{x_p(\frac{1}{2} + \frac{u}{2}p^{-\frac{1}{3}}) - \sqrt{p}}{p^{-\frac{1}{6}}} \equiv \mathcal{A}_2(u) - u^2 \quad (1)$$

where  $\mathcal{A}_2(u)$  is the Airy<sub>2</sub> process [8] which is a stationary, and non-Markovian, process. In particular,  $\text{Proba}[\mathcal{A}_2(0) \leq \xi] = \mathcal{F}_2(\xi)$ . In this Letter, we compute exactly the joint distribution  $P_p(M, \tau_M)$  of the maximal height  $M$  and its position  $\tau_M$  for the vicious walker problem (Fig. 1 c)). While the maximal height  $M$  has been recently studied [25, 26], nothing is known about the distribution of  $\tau_M$ , which has by the way recently attracted much interest in various other one-dimensional stochastic processes [27–30]. Our results are not only relevant, for finite  $p$ , for the vicious walkers problem, but thanks to the above relation (1), become exact for  $p \rightarrow \infty$ , for curved growing interface, as well as for the DPRM. We actually show that for moderate values of  $p \sim 10$ , our analytical formula describes quite accurately our numerical data for the PNG model.

**Method.** – The basic idea of the method to compute  $P_p(M, \tau_M)$  is to divide the “watermelons” configuration in two time intervals,  $\tau \in [0, \tau_M]$  and  $\tau \in [\tau_M, 1]$  and use the Markov property of the whole process to treat these two intervals independently (Fig. 1 d)). In both intervals, the  $p$  vicious walkers are constrained to stay below  $M$ , while we impose  $x_p(\tau_M) = M$ . To compute the propagator of these constrained vicious walkers in each sub-interval, we use a path-integral approach. Let us denote  $p_{<M}(\mathbf{b}, t_b | \mathbf{a}, t_a)$  the propagator of  $p$  non-intersecting Brownian motions, starting in  $\mathbf{a} \equiv (a_1, \dots, a_p)$  at time  $t_a$  and ending in  $\mathbf{b} \equiv (b_1, \dots, b_p)$  at time  $t_b$  and constrained to stay below  $M$  in the time interval  $[t_a, t_b]$ .  $p_{<M}(\mathbf{b}, t_b | \mathbf{a}, t_a)$  is given by the sum of the weights  $\exp\left[-\frac{1}{2} \sum_{i=1}^p \int_{t_a}^{t_b} \left(\frac{dx_i}{d\tau}\right)^2 d\tau\right]$  over all trajectories satisfying  $x_1(\tau) < x_2(\tau) < \dots < x_p(\tau) < M$ , for  $\tau \in [t_a, t_b]$ . In the language of path integrals, this corresponds to the propagator (in imaginary time) of  $p$  quantum free fermions with an infinite wall in  $x = M$ , the associated Schrödinger Hamiltonian being  $H_M = -\frac{1}{2} \sum_{i=1}^p \partial_{x_i}^2 + V_M(x)$ . The hard wall potential is given by  $V_M(x) = 0$  if  $x < M$  and  $V_M(x) = +\infty$  if  $x > M$  [25]. The use of fermions incorporates naturally the non-colliding condition [25, 31, 32]. This allows to write this propagator as

$$p_{<M}(\mathbf{b}, t_b | \mathbf{a}, t_a) = \langle \mathbf{b} | e^{-(t_b - t_a)H_M} | \mathbf{a} \rangle, \quad (2)$$

which we can compute using a spectral decomposition over the fermionic eigenfunctions of  $H_M$ . Before doing this, we notice that the “watermelons” configurations that we study here are actually ill-defined for Brownian motions which are continuous both in space and time. It is indeed well known that if two walkers cross each other they will recross each infinitely many times immediately after

the first crossing. This means in particular that it is impossible to impose  $x_i(0) = x_{i+1}(0)$  and simultaneously  $x_i(0^+) < x_{i+1}(0^+)$ . Here, following Ref. [19, 25, 27], we adopt a regularization scheme where we impose that the  $p$  walkers start and end at  $0 < \epsilon < \dots < (p-1)\epsilon$  and take eventually the limit  $\epsilon \rightarrow 0$ . We use an additional cut-off procedure by imposing that  $x_p(\tau_M) = M - \eta$  and then take the limit  $\eta \rightarrow 0$ .

**Results for  $p$  vicious walkers.** – The calculation of  $P_p(M, \tau_M)$  requires the computation of  $p_{<M}(\mathbf{b}, t_b | \mathbf{a}, t_a)$ . Expanding Eq. (2) over the fermionic eigenvectors of  $H_M$  yields

$$p_{<M}(\mathbf{b}, t_b | \mathbf{a}, t_a) = \langle \mathbf{b} | e^{-(t_b - t_a) H_M} | \mathbf{a} \rangle \\ = \int_0^\infty d\mathbf{k} e^{-\frac{\mathbf{k}^2}{2}(t_b - t_a)} \det_{1 \leq i, j \leq p} \phi_{k_i}(b_j) \det_{1 \leq i, j \leq p} \phi_{k_i}^*(a_j), \quad (3)$$

where  $\phi_k(x) = \sqrt{\frac{2}{\pi}} \sin[k(M-x)]$  naturally appear as the eigenvectors of  $H_M$  and where we use the notations  $\int_0^\infty d\mathbf{k} \equiv \int_0^\infty dk_1 \dots \int_0^\infty dk_p$  and  $\mathbf{k}^2 = k_1^2 + \dots + k_p^2$ . In Eq. (3), the determinants appear as Slater determinants in the associated fermions problem. From this propagator (3) we compute  $P_p(M, \tau_M)$  by dividing the configuration in two time independent intervals,  $\tau \in [0, \tau_M]$  and  $\tau \in [\tau_M, 1]$  as explained above (see also Fig. 1 d)) to obtain:

$$P_p(M, \tau_M) = \lim_{\epsilon, \eta \rightarrow 0} \frac{1}{Z_p} \int_{-\infty}^{M-\eta} d\mathbf{y} p_{<M}(\epsilon, 1 | \mathbf{y}, \tau_M) \\ \times p_{<M}(\mathbf{y}, \tau_M | \epsilon, 0) \delta(y_p - (M - \eta)), \quad (4)$$

where the delta function enforces  $x_p(\tau_M) = M - \eta$  and where the amplitude  $Z_p$ , which depends explicitly on  $\epsilon$  and  $\eta$  is determined by the normalization condition  $\int_0^{+\infty} dM \int_0^1 d\tau_M P_p(M, \tau_M) = 1$ . Using the above formula for the constrained propagator (3) in Eq. (4), and taking the limits  $\epsilon, \eta \rightarrow 0$  one obtains

$$P_p(M, \tau_M) = z_p^{-1} M^{-(p^2+3)} \int_0^\infty d\mathbf{q} \int_0^\infty dq'_p e^{-\frac{\sum_{i=1}^{p-1} q_i^2}{2M^2}} \\ \times e^{-\frac{\tau_M q_p^2 + (1-\tau_M) q'_p{}^2}{2M^2}} q_p q'_p \Theta_p(q_1, \dots, q_p) \Theta_p(q_1, \dots, q'_p), \quad (5)$$

where  $\Theta_p(\mathbf{q})$  is the following determinant

$$\Theta_p(\mathbf{q}) = \det_{1 \leq i, j \leq p} q_i^{j-1} \cos(q_i - j\pi/2). \quad (6)$$

To compute  $z_p$ , we use that  $\int_0^1 P_p(M, \tau_M) d\tau_M$  must yield back the expression for the distribution of the maximum as computed in Ref. [25]. This allows to obtain  $z_p = \pi^{1+\frac{p}{2}} 2^{-\frac{3p}{2}} \prod_{j=0}^{p-1} j!$ . In Eq. (5), one can expand the determinant by minors and then perform the integrals over  $q_i$  using the Cauchy-Binet identity which reads

$$\int d\mathbf{x} \det_{1 \leq i, j \leq p} f_i(x_j) \det_{1 \leq i, j \leq p} g_i(x_j) \\ = p! \det_{1 \leq i, j \leq p} \int dx f_i(x) g_j(x), \quad (7)$$

for any suitable functions  $f_i(x)$  and  $g_i(x)$ . These integrals can be expressed in terms of Hermite polynomials  $H_n(x)$  and we obtain finally

$$P_p(M, \tau_M) = B_p[\det D] {}^t U(\tau_M) D^{-1} U(1 - \tau_M), \quad (8)$$

with  $B_p^{-1} = (2\pi)^{\frac{1}{2}} \prod_{j=0}^{p-1} (j! 2^j)$  and where  $D \equiv D(M)$  is a  $p \times p$  matrix

$$D_{i,j} = (-1)^{i-1} H_{i+j-2}(0) - e^{-2M^2} H_{i+j-2}(\sqrt{2}M), \quad (9)$$

while  $U(\tau) \equiv U(M, \tau)$  is a column vector given by

$$U_i(\tau) = \tau^{-\frac{i+1}{2}} H_i\left(\frac{M}{\sqrt{2}\tau}\right) e^{-\frac{M^2}{2\tau}}. \quad (10)$$

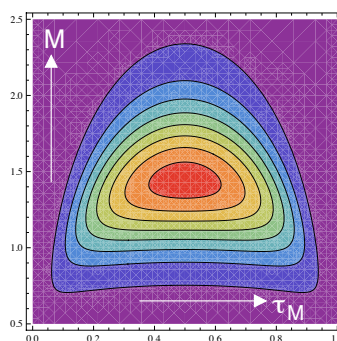


Fig. 2: Contour plot of  $P_p(M, \tau_M)$  for  $p = 3$ . The contour lines correspond to 0.1, 0.4,  $\dots$ , 2.2.

In Fig. (2), we show a contour plot of  $P_p(M, \tau_M)$  for  $p = 3$ . For fixed  $\tau_M \in [0, 1]$ ,  $P_p(M, \tau_M)$ , as a function of  $M$  has a simple bell shape. Its behavior for fixed value of  $M$  as a function of  $\tau_M$  is more interesting. For sufficiently large  $M > M_p^*$ , it has a bell shape, with a maximum in  $\tau_M = \frac{1}{2}$ , while for  $M < M_p^*$ , it has a "M-shape" with two distinct maxima,  $\tau_M = \frac{1}{2}$  being a local minimum. One observes that  $M_p^*$  is a slowly increasing function of  $p$ .

By integrating our expression in Eq. (8) over  $\tau_M$ , one checks that we recover the formula for the pdf of  $M$ , as obtained in Ref. [26]. Indeed, one finds  $\text{Proba}[\max_\tau x_p(\tau) \leq M] = \det D / \prod_{j=0}^{p-1} (j! 2^j)$ , where the matrix  $D$  is defined in Eq. (9). On the other hand, by integrating Eq. (8) over  $M$ , one obtains an expression for  $P_p(\tau_M)$ . While for  $p = 1$ ,  $P_1(\tau_M) = 1$ , one obtains, for instance, for  $p = 2$

$$P_2(\tau_M) = 4 \left( 1 - \frac{1 + 10\tau_M(1 - \tau_M)}{(1 + 4\tau_M(1 - \tau_M))^{5/2}} \right). \quad (11)$$

For generic  $p$ ,  $P_p(\tau_M)$  is a function of  $\tau_M(1 - \tau_M)$  with the asymptotic behavior, for small  $\tau_M$

$$P_p(\tau_M) \sim \tau_M^{\nu(p)}, \quad \text{with } \nu(p) = (p^2 + p - 2)/2. \quad (12)$$

Note that for  $p$  independent Brownian motions (without the non-crossing condition) one has  $P_{p,\text{free}}(\tau_M) \sim \tau_M^{p-1}$  [29] so that the exponent  $\nu(p)$  bears the signature of the non-colliding condition.

The above approach can be extended to study the extreme statistics of  $p$  non-intersecting excursions, *i.e.* vicious walkers starting and terminating at the origin but with the additional constraint that they all stay positive inbetween [25, 33, 34]. The slight modification in our computation is to replace the Hamiltonian  $H_M$  (with a wall in  $x = M$ ) with the box Hamiltonian  $H_{\text{Box}}$  (with two walls: in  $x = 0$  and in  $x = M$ ). Hence the energy levels are discrete, and consequently one has to treat discrete sums instead of integrals as before. Using the appropriate propagator in Eq. (4), one finds, taking the limits  $\epsilon, \eta \rightarrow 0$ , the joint pdf for the non-intersecting excursions

$$P_{p,E}(M, \tau_M) = z_{p,E}^{-1} M^{-(2p^2+p+3)} \sum_{n_1, \dots, n_p, n'_p > 0} (-1)^{n_p+n'_p} e^{-\frac{\pi^2}{2M^2} [\sum_{i=1}^{p-1} n_i^2 + \tau_M n_p^2 + (1-\tau_M) n'_p{}^2]} \times \prod_{i=1}^{p-1} n_i^2 n_p^2 n'_p{}^2 \Delta_p(n_1^2, \dots, n_p^2) \Delta_p(n_1^2, \dots, n'_p{}^2), \quad (13)$$

where we use the notation  $\Delta_p(\lambda_1, \dots, \lambda_p) = \prod_{1 \leq i < j \leq p} (\lambda_j - \lambda_i)$  for the Vandermonde determinant, and with the normalization  $z_{p,E} = 2^{\frac{p^2}{2}} \Gamma(p) \prod_{j=0}^{p-1} (2^j j! \Gamma(\frac{3}{2} + j)) \pi^{-(2p^2+p+2)}$ . Performing similar manipulations as before, one finds the joint pdf of the couple  $(M, \tau_M)$  for the excursions configuration in a determinantal form, reminiscent of the watermelons case (8):

$$P_{p,E}(M, \tau_M) = C_p [\det D_E] {}^t U_E(\tau_M) D_E^{-1} U_E(1 - \tau_M), \quad (14)$$

with  $C_p^{-1} = (-1)^{p+1} 2^{2p^2-\frac{1}{2}} \prod_{j=1}^{p-1} (j! \Gamma(\frac{3}{2} + j)) \pi^{-1}$ . The  $p \times p$  matrix  $D_E \equiv D_E(M)$  is (for  $1 \leq i, j \leq p$ )

$$D_{Ei,j} = \sum_{n=-\infty}^{+\infty} H_{2(i+j-1)}(\sqrt{2}Mn) e^{-2M^2 n^2}, \quad (15)$$

and appears in the expression of the cumulative distribution of the maximum [33],  $\text{Proba}[\max_{\tau} x_p(\tau) \leq M] = (-1)^p \det D_E / (2^{p^2} \prod_{j=1}^p (2j-1)!)$ . The vector elements are (for  $i = 1, \dots, p$ )

$$U_{Ei}(\tau) = \frac{1}{M} \left( -\frac{2\pi^2}{M^2} \right)^i \sum_{n=1}^{\infty} (-1)^n n^{2i} e^{-\frac{2\pi^2}{M^2} n^2 \tau}. \quad (16)$$

The integration of formula (13) with respect to  $M$  gives the pdf of the time to reach the maximum in this excursion process. For  $p = 1$ , the formula in Eq. (13) yields back the result obtained in Ref. [27]. For  $p = 2$ , we give the expression of  $P_{2,E}(\tau_M)$

$$P_{2,E}(\tau_M) = a \sum_{n_i > 0} \frac{(-1)^{n_2+n_3} n_1^2 n_2^2 n_3^2 (n_1^2 - n_2^2)(n_1^2 - n_3^2)}{(n_1^2 + \tau_M n_2^2 + (1 - \tau_M) n_3^2)^6}, \quad (17)$$

with  $a = 1280/\pi$ .

### Application to stochastic growth processes. –

We now come back to the joint pdf  $P_t(M, X_M)$  for curved growing interfaces (Fig. 1 a)). From Eq. (1) one obtains

$$P_t(M, X_M) \sim t^{-1} \mathcal{P}_{\text{Airy}}((M-2t)t^{-\frac{1}{3}}, X_M t^{-\frac{2}{3}}) \quad (18)$$

where  $\mathcal{P}_{\text{Airy}}(y, x)$  is the joint distribution of the maximum  $y$  and its position  $x$  for the process  $\mathcal{A}_2(u) - u^2$ ,  $u \in \mathbb{R}$ . From Ref. [16, 21, 22] one obtains that the (marginal) pdf of  $y$ ,  $\mathcal{P}_{\text{Airy},M}(y)$ , is given by TW,  $\mathcal{P}_{\text{Airy},M}(y) = \mathcal{F}'_1(y)$ , and hence  $P_t(M) \sim t^{-\frac{1}{3}} \mathcal{F}'_1((M-2t)/t^{\frac{1}{3}})$ . On the other hand, from Eq. (1),  $\mathcal{P}_{\text{Airy}}(y, x)$  can be obtained from our results for  $P_p(M, \tau_M)$  in Eq. (8): in the scaling limit  $y = (M - \sqrt{p})p^{\frac{1}{6}}$  as well as  $x = 2(\tau_M - \frac{1}{2})p^{\frac{1}{3}}$  fixed one has indeed  $P_p(M, \tau_M) \sim 2p^{\frac{1}{2}} \mathcal{P}_{\text{Airy}}(y, x)$ . While our expression (8) should be amenable to an asymptotic analysis for large  $p$ , yielding an explicit exact expression for  $\mathcal{P}_{\text{Airy}}(y, x)$ , such an analysis deserves further investigations. Here we show instead that, for finite values of  $p$ , this expression (8) describes quite accurately our numerical data for the extreme statistics of the PNG model in the droplet geometry. To illustrate this, we have computed numerically the (marginal) distribution of the position of the maximum  $X_M$ . We recall that, for the DPRM as in Fig. (1 b)),  $X_M$  is the position of the free end of the optimal polymer.

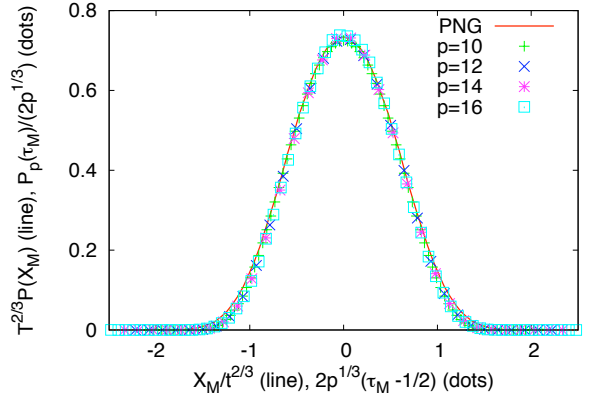


Fig. 3: On linear scales, the solid line is a plot of  $t^{\frac{2}{3}} P_t(X_M)$  as a function of  $X_M/t^{\frac{2}{3}}$ , for  $t = 768$ , computed numerically for the PNG, while the dots correspond to our analytical results  $P_p(\tau_M)/(2p^{\frac{1}{3}})$  (8) as a function of  $2p^{\frac{1}{3}}(\tau_M - \frac{1}{2})$  for  $p = 10, 12, 14$  and  $p = 16$ .

In Fig. 3, we show a plot of the rescaled distribution  $t^{\frac{2}{3}} P_t(X_M/t^{\frac{2}{3}})$  as a function of the rescaled variable  $X_M/t^{\frac{2}{3}}$  for  $t = 768$  in solid line. We also plot our exact analytical results for watermelons, *i.e.*  $P_p(\tau_M)/(2p^{\frac{1}{3}})$  as a function of  $(2p^{\frac{1}{3}}(\tau_M - \frac{1}{2}))$  for  $p = 10, 12, 14$  and  $16$  which is computed from Eq. (8) as  $P_p(\tau_M) = \int_0^\infty dM P_p(M, \tau_M)$ . We

emphasize that the good collapse of the different curves is obtained without any fitting parameter.

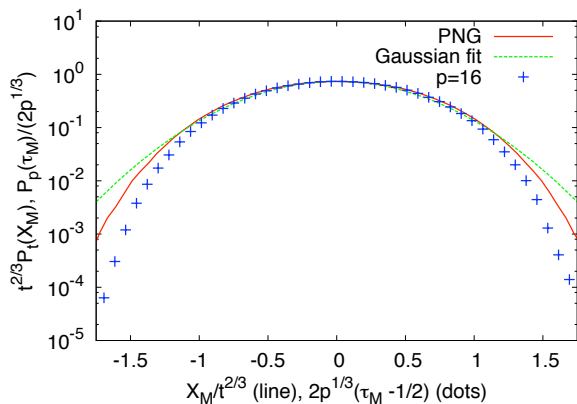


Fig. 4: Log-linear plot of: the rescaled distribution of the position of the maximum for PNG (solid line), the rescaled distribution of the time to reach the maximum for the  $p = 16$  watermelons configuration (dots), and the closest Gaussian curve (dashed line), that do not match the PNG curve. The scaled quantities appears in the  $x, y$  labels (and are detailed in the caption of Fig 3).

In Fig. 4, we show a plot of the same quantities as in Fig. 3 in log-linear plot. As expected, one observes some deviations between the result for the PNG and our computation for finite  $p = 16$  in the tail of the distribution. Besides, our numerical data suggest that the marginal distribution of  $X_M$  is *non-Gaussian* (the best Gaussian approximation being shown as a dotted line). Instead, for  $X_M \gg t^{2/3}$ , our data are compatible with a stretched exponential behavior  $P_t(X_M) \sim t^{-\frac{2}{3}} e^{-\gamma \left(\frac{X_M}{t^{2/3}}\right)^\delta}$  with  $\delta \simeq 2.5$  while its precise determination requires more numerical efforts. Interestingly, for  $p$  free Brownian bridges, one can show [29] that the distribution of  $\tau_M$  converges to a Gaussian distribution centered in  $\frac{1}{2}$  of width  $(8 \log n)^{-\frac{1}{2}}$ . Therefore, the non-Gaussianity of  $P_t(X_M)$  is a clear signature of the correlations in the associated vicious walkers problem.

The results obtained in the present Letter extend far beyond the PNG model. Indeed our results hold more generally for stochastic growth models, and physical situations, where the interface  $h(x, t)$  at point  $x$  and time  $t$  evolves according to the one-dimensional KPZ equation [5]

$$\frac{\partial}{\partial t} h(x, t) = \nu \nabla^2 h(x, t) + \frac{\lambda}{2} (\nabla h(x, t))^2 + \zeta(x, t), \quad (19)$$

in a curved geometry. In Eq. (19),  $\zeta(x, t)$  is a Gaussian white noise of zero mean and correlations  $\langle \zeta(x, t) \zeta(x', t') \rangle = D \delta(x - x') \delta(t - t')$ . In Ref. [8], it was shown that the fluctuations of physical observables

of the height field, evolving according to Eq. (19), are universal, up to two non-universal parameters  $\lambda$  and  $A = D/2\nu$ . Once  $\lambda$  and  $A$  are fixed, these fluctuations are characterized by universal distribution functions. In the curved geometry,  $\lambda$  can be simply measured as the radial growth rate,  $\langle h(x = 0, t) \rangle \sim \lambda t$  while  $A$  can be extracted from the width of the interface  $\langle (h(0, t) - \langle h(0, t) \rangle)^2 \rangle^{1/2} \sim AL/6$  for a system of finite size  $L$  [21]. For instance, the fluctuations of the height field are given by  $h(0, t) \simeq \lambda t + (A^2 \lambda t / 2)^{1/3} \chi_{\text{GUE}}$  where  $\chi_{\text{GUE}}$  is a random variable distributed according to the TW distribution  $\mathcal{F}_2$  [8]. This universality was convincingly demonstrated in recent experiments [13]. Therefore, for an interface described by the KPZ equation (19) in a droplet geometry, one expects that the distribution of the position of the maximum  $X_M$  will have the scaling form  $P_t(X_M) \sim \xi(t)^{-1} \mathcal{P}_{\text{Airy}, X_M}(X_M / \xi(t))$  with  $\xi(t) = (2/A)(A^2 \lambda t / 2)^{2/3}$  is the correlation length. The scaling function  $\mathcal{P}_{\text{Airy}, X_M}(x)$  is universal and can be computed from our formulas in Eq. (8, 18), see also Fig. 3.

**Conclusion.** – To conclude, we have obtained an exact expression for the joint distribution of the maximum  $M$  and the time  $\tau_M$  at which this maximum is reached for  $p$  non-intersecting Brownian bridges (8) and excursions (14). We have shown that our analytic expression for moderate values of  $p$  Brownian bridges describe very accurately the extreme statistics of curved growing interfaces, becoming eventually exact in the limit  $p \rightarrow \infty$ . In addition to their relevance to the DPRM, our results may have applications to various other situations like step fluctuations in faceted crystals [35] or dimer-covering problems [36], where it was shown that the fluctuations are governed by the very same process  $\mathcal{A}_2(u) - u^2$  that we have studied here. Finally, in view of recent progresses [12, 13], it seems possible to observe these extremal statistics for curved growing interfaces in experimental situations like nematic liquid crystals [13].

\*\*\*

We thank T. Sasamoto for useful correspondence.

## REFERENCES

- [1] J. Krug, H. Spohn, in *Solids far from equilibrium* (ed. by C. Godrèche), Cambridge Univ. Press, New York (1991).
- [2] T. Halpin-Healy, Y.C. Zhang, Phys. Rep. **254**, 215 (1995).
- [3] S.V. Khare, T.L. Einstein, Phys. Rev. B **54**, 11752 (1996).
- [4] A. Brú, J. M. Pastor, I. Feraud, I. Brú, S. Melle, and C. Berenguer, Phys. Rev. Lett. **81**, 4008 (1998).
- [5] M. Kardar, G. Parisi, Y.-C. Zhang, Phys. Rev. Lett. **56**, 889 (1986).
- [6] T. Sasamoto, H. Spohn, Phys. Rev. Lett. **104**, 230602 (2010).
- [7] D. Dhar, Phase Transitions **9**, 51 (1987); L.-H. Gwa, H. Spohn, Phys. Rev. Lett. **68**, 725 (1992).

- [8] M. Prähofer, H. Spohn, Phys. Rev. Lett. **84**, 4882 (2000); J. Stat. Phys., **108**, 1071 (2002).
- [9] K. Johansson, Comm. Math. Phys. **209**, 437 (2000); J. Gravner, C. A. Tracy and H. Widom, J. Stat. Phys. **102**, 1085 (2001); S. N. Majumdar, S. Nechaev, Phys. Rev. E **69**, 011103 (2004).
- [10] S. N. Majumdar, *Les Houches Lecture Notes on "Complex Systems"*, 2006 ed. by J.P. Bouchaud, M. Mézard and J. Dalibard.
- [11] C. A. Tracy, H. Widom, Comm. Math. Phys. **159**, 151 (1994); *ibid.* **177**, 727 (1996).
- [12] L. Miettinen, M. Myllys, J. Merikoski and J. Timonen, Eur. Phys. J. B **46**, 55 (2005).
- [13] K.A. Takeuchi, M. Sano, Phys. Rev. Lett. **104**, 230601 (2010).
- [14] F.C. Franck, J. Cryst. Growth **22**, 233 (1974); J. Krug, H. Spohn, Europhys. Lett. **8**, 219 (1989).
- [15] M. Prähofer, Ph. D thesis, Ludwig-Maximilians-Universität, München, 2003.
- [16] K. Johansson, Comm. Math. Phys. **242**, 277 (2003).
- [17] V. Dotsenko, B. Klumov, J. Stat. Mech. (2010) P03022; P. Calabrese, P. Le Doussal, A. Rosso, Europhys. Lett. **90**, 20002 (2010); G. Amir, I. Corwin, J. Quastel, arXiv:1003.0443.
- [18] S. Raychaudhuri, M. Cranston, C. Przybyla, and Y. Shapir, Phys. Rev. Lett. **87**, 136101 (2001).
- [19] S. N. Majumdar, A. Comtet, Phys. Rev. Lett. **92**, 225501 (2004); J. Stat. Phys. **119**, 777 (2005).
- [20] G. Schehr, S. N. Majumdar, Phys. Rev. E **73**, 056103 (2006); G. Györgyi, N. R. Moloney, K. Ozogány, and Z. Rácz, Phys. Rev. E **75**, 021123 (2007); T. W. Burkhardt, G. Györgyi, N. R. Moloney, and Z. Rácz, Phys. Rev. E **76**, 041119 (2007); J. Rambeau, G. Schehr, J. Stat. Mech., P09004 (2009).
- [21] J. Krug, P. Meakin, T. Halpin-Healy, Phys. Rev. A **45**, 638 (1992).
- [22] J. Baik, E.M. Rains, in *Random matrix models and their applications*, MSRI Publications **40**, Cambridge Univ. Press (2001).
- [23] M. E. Fisher, J. Stat. Phys. **34**, 667 (1984).
- [24] P. Ferrari, Lecture Notes of Beg-Rohu Summer School, available at <http://ipht.cea.fr/Meetings/BegRohu2008/>.
- [25] G. Schehr, S. Majumdar, A. Comtet, and J. Randon-Furling, Phys. Rev. Lett. **101**, 150601 (2008).
- [26] T. Feierl, Proc. of IWOCA 2009, *Lecture Notes in Computer Science*, vol. 5874 (2009).
- [27] S. Majumdar, J. Randon-Furling, M. Kearney, and M. Yor, J. Phys. A: Math. Theor. **41**, 365005 (2008).
- [28] G. Schehr, P. Le Doussal, J. Stat. Mech. P01009 (2010); S. N. Majumdar, A. Rosso, A. Zoia, J. Phys. A: Math. Theor. **43**, 115001 (2010).
- [29] J. Randon-Furling, S. N. Majumdar, A. Comtet, Phys. Rev. Lett. **103**, 140602 (2009); S. N. Majumdar, A. Comtet, J. Randon-Furling, J. Stat. Phys. **138**, 955 (2010)
- [30] S. N. Majumdar, A. Rosso, A. Zoia, Phys. Rev. Lett. **104**, 020602 (2010).
- [31] C. Nadal, S.N. Majumdar, Phys. Rev. E **79**, 061117 (2009).
- [32] P.G. de Gennes, J. Chem. Phys. **48**, 2257 (1968).
- [33] M. Katori, M. Izumi and N. Kobayashi, J. Stat. Phys. **131**, 1067 (2008); N. Kobayashi, M. Izumi, M. Katori, Phys. Rev. E **78** 051102 (2008).
- [34] T. Feierl, Proc. of the AofA2007, DMTCS Proc. (2007).
- [35] P.L. Ferrari, H. Spohn, J. Stat. Phys. **113**, 1 (2003).
- [36] K. Johansson, Probab. Theory Rel. **123**, 225 (2002).